Estimating Wave Attenuation at the Coastal Land Margin with a GIS Toolbox

Madeline R. Foster-Martinez[a,1]*, Karim Alizad[b], Scott C. Hagen[a,c,d]

[a] Center for Coastal Resiliency, Louisiana State University; 124B Sea Grant, Baton Rouge, LA 70803, US
[b] Belle W. Baruch Institute for Marine and Coastal Sciences, University of South Carolina; Columbia, SC 29208, US
[c] Department of Civil and Environmental Engineering, Louisiana State University; 3255 Patrick F. Taylor, Baton Rouge, LA 70803, US
[d] Center for Computation and Technology, Louisiana State University; 1079 Digital Media Center Baton Rouge, LA 70803, US

*corresponding author, Telephone: +1 504-782-2172

Email addresses: M.R. Foster-Martinez (mrfoster@uno.edu); K. Alizad (alizad@sc.edu); S.C. Hagen (sha-gen@lsu.edu)

[1]Present address: Pontchartrain Institute for Environmental Sciences, University of New Orleans; 2000 Lakeshore Drive; Rm 1036 Geology-Psychology; New Orleans, LA 70148, US

Abstract

Wave attenuation is a key process that impacts activities at the coastal land margin and is an ecosystem service provided by many natural landscapes. Traditional modelling tools for wind wave attenuation require advanced expertise to apply. We present an alternative, GIS-based option for estimating wave attenuation, the Wave Attenuation Toolbox (WATTE). The outputs are a map of wave height transmission as a percentage of the original wave height and a line demarking the extent of wave exposure onshore. WATTE supports a variety of inputs, ranging from outputs of ecological and landscape evolution models to remote sensing data, and past, present, and future conditions can be analyzed. The present version of WATTE models wave attenuation as an exponential decay process, and a recommendation table for exponential decay constants is derived from previous studies. Three examples of applying WATTE to marsh environments are described.

Key Words

Wave attenuation; GIS toolbox; Coastal process; Marsh; Ecosystem services; Participatory modeling

Software Availability

Name: Wave Attenuation Toolbox
Developer: M. Foster-Martinez (contact information above)
Year: 2020
Software required: ArcMap 10.3 or later with Spatial Analyst extension. Optional features require the Advanced license.
Language: Python
Size: 32 KB
Availability: A digital object identifier (DOI) will be assigned to the toolbox code, and the code will be made publicly available on Github (GNU General Public License v3) if the manuscript is accepted for publication.
Cost: Free

1. Introduction

Wind-waves largely determine the form and function of the coastal land margin. About half the total energy for all natural coastal processes (*i.e.* biological, chemical, and physical processes) come from waves (Leigh et al., 1987; Short, 2012). Wave energy is dissipated in the nearshore primarily through breaking and encountering frictional elements. Natural coastal ecosystems and structures attenuate wave action, including mangroves (Abuodha & Kairo, 2001; Ilman et al., 2016), coral reefs (Hughes et al., 2018), seagrass beds (Guannel et al., 2016; Waycott et al., 2009), marshes (Crosby et al., 2016; K. Bromberg Gedan et al., 2009; Gedan et al., 2011), and oyster reefs (Wiberg et al., 2018). Anthropogenic activity has indirectly and directly altered the patterns of wave energy. Marine structures (*e.g.* breakwaters, sea walls, revetments, etc.) directly prevent wave penetration in some areas, while enhancing wave reflection and increasing wave energy in others (Reeve et al., 2018). Land conversion for shoreline development and the effects of climate change have damaged and decreased the area of vegetated coastal ecosystems by as much as 50% since mid-twentieth century (Duarte et al., 2013). At the same time, the use of natural and nature-based features (NNBFs) for coastal protection is gaining recognition for being cost-effective and providing multiple benefits (Bridges et al., 2015; Narayan et al., 2016; Sutton-Grier & Sandifer, 2018). As changes in the coastal land margin continue to occur, it is important to understand and communicate the impacts on wave energy.

Here, we have created a Geographic Information Systems (GIS) toolbox that estimates and maps wave attenuation. The present version of the toolbox is built for estimating wave attenuation through marshes; however, it could be readily adapted to other coastline types (*e.g.* mangroves, seagrass beds, kelp forests). The toolbox leverages existing datasets from a range of sources including remote sensing and coastal landscape evolution models, allowing for analysis of past, present, and future conditions. By using a simple algorithm, the toolbox does not require advanced expertise to apply and remains accessible to a range of stakeholder groups *(e.g.* local resource managers, agencies, and non-profits*).* The following sections provide background on wave attenuation and modeling tools and describe the toolbox algorithm. We present three examples that illustrate potential uses of the toolbox, followed by discussion and conclusions.

2. Background

2.1. Wave Attenuation through Marsh Vegetation: Processes, Measurement, and Modeling

Wave energy is a function of wave height (*i.e.* the vertical distance between the crest and trough of a wave); waves with larger wave heights have greater energy. As waves move onshore, many dissipative processes are at work, such as wave breaking and friction due to bottom roughness, but on healthy vegetated shorelines, encountering vegetation is the primary energy dissipation mechanism under normal conditions (*i.e.* non-storm) (Guannel et al., 2015; I. Möller et al., 1999). Vegetation has the greatest impact on waves with shorter wave periods (*i.e.* < 1 min) (Paquier et al., 2016; van Rooijen et al., 2016), which include wind-generated sea-swell and infragravity waves (Munk, 1950).

The amount waves are attenuated across a marsh can vary greatly between sites or even at the same site under different conditions (Koch et al., 2009; Pinsky et al., 2013). Greater attenuation is observed when vegetation occupies a greater proportion of the water column, which can be due to increased stem density, width, or height (Peruzzo et al., 2018). That proportion can change over the course of a tidal cycle, as the ratio of the water depth to vegetation height changes, or between vegetation patches with varying characteristics (*e.g.* stem density, width, and stiffness). Therefore, a range of attenuation that can be expected at a site is more meaningful than one single value.

Field measurements of wave attenuation through marshes measure wave heights at multiple points along a transect perpendicular to the shoreline (*e.g.* Jadhav & Chen, 2013; I. Möller & Spencer, 2002). With known locations of instruments, the decrease in wave height per unit length along the transect can be calculated. Underlying this method is the assumption that wave refraction causes the waves to cross the marsh parallel to the shoreline (Komar, 1998).

The way wave attenuation is modeled depends on the application. Here, we chose to model it as an exponential decay (Kobayashi et al., 1993):

$$W_T = H_1/H_0 = e^{-kx} \quad \text{(Eq. 1)}$$

Where W_T is the fraction of wave height transmission; H is wave height; 1 and 0 subscripts denote the location closer to onshore and offshore, respectively; k is the exponential decay constant; and x is the cross-shore distance between H_1 and H_0. This model requires minimal input (*i.e.* only k) and describes field measurements well (Tempest et al., 2015 and references therein).

There are multiple other hydrodynamic models that include the effects of vegetation with varying levels of complexity and applicable spatial scales. Large-scale models typically represent vegetation as bottom

friction and parameterize it via Manning's n (*e.g.* ADCIRC (Luettich Jr et al., 1992)). This representation is appropriate for storm surge but is not as useful for wind waves, where vegetation is more directly impactful. Models that do address wind wave-vegetation interaction often model vegetation as a drag force, as originally described by Dalrymple et al. (1984). Examples include XBeach-VEG (Roelvink et al., 2009; van Rooijen et al., 2015), SWAN-VEG (Simulating Waves Nearshore-Vegetation (Suzuki et al., 2012)), and the InVEST (Integrated Valuation of Ecosystem Services and Tradeoffs) Coastal Protection model (Guannel et al., 2015). These models require a drag coefficient for the vegetation, which has been shown to vary with hydrodynamic conditions (*e.g.* Reynolds number (Möller et al., 2014) and Keulegan–Carpenter number (Jadhav & Chen, 2013)). Other required inputs include vegetation parameters (*e.g.* stem count) and wave parameters (*e.g.* wave number and height). Most of these models operate on a mesh grid and need advanced expertise to run. They can be run to simulate past, present, or future conditions (*e.g.* Hijuelos et al., 2019). The GIS toolbox presented in this paper is in no way intended to replace any of the aforementioned models, but rather, it is a simpler alternative that may be more suitable for some communities' modeling and information needs.

2.2. Related Tools for Coastal Planning

Method frameworks have been created specifically for the assessment of natural systems for coastal protection. For example, Osorio-Cano et al. (2017) describe a four stage process, beginning with parameterization of the natural system and ending with a coastal management plan. The framework includes an assessment of wave attenuation using advanced numerical models (*e.g.* XBeach (Roelvink et al., 2010)). Similarly, van Zanten et al. (2014) present a framework that uses information on the wave attenuation capacity of coral reefs to calculate their coastal protection value. For both frameworks, a lack of site data or of model expertise could prevent a user group from completing the critical step of assessing wave attenuation capacity and progressing in the framework.

The Coastal Protection Nearshore Wave and Erosion module of InVEST (Guannel et al., 2015; Tallis et al., 2010) provides a framework and toolboxes that operate in a GIS environment. InVEST estimates the value of coastal protection services for a range of coastal environments (*e.g.* Doughty et al., 2017; Ruckelshaus et al., 2016) by using the damage averted (*i.e.* erosion) to assess value. It produces wave attenuation estimates along a single cross-shore transect and requires detailed information, such as cross-shore bathymetry and wave parameters, to run. Since its initial development, InVEST has evolved,

and this module is no longer being maintained by developers. However, the broad use of the module demonstrates the overall need for this type of information.

3. Methods

This paper describes the **W**ave **Atte**nuation (WATTE) Toolbox, a custom ArcGIS toolbox that is run within ArcMap (*ArcGIS*, 2018). The code is open source and available for download (*note to editor and reviewers: a DOI for the code will be available through Github after publication acceptance*). The present version of WATTE estimates the decrease in wave height that occurs as waves cross though marsh vegetation using an exponential wave decay formulation (*i.e.* Eq. 1). WATTE uses an image of the region of interest and simulates a process similar to how wave attenuation is measured in the field. The output is an estimate of wave height transmission throughout the entire marsh.

3.1. Toolbox Algorithm

WATTE executes the following steps, which are illustrated in Figure 1.

- Inputs: The main inputs are a raster of the area of interest classified by land type (Figure 1a) and exponential decay constants for each marsh classification.

1. Identify the marsh-water interface: Each cell classification in the raster is converted to a polygon, and the edges of the polygons are converted to polylines. A new line, the marsh-water interface line, is created where marsh and water polylines intersect (black line Figure 1b).
2. Draw cross-shore transects: Transects, polyline features, are drawn perpendicular to the marsh-water interface line, extending in both onshore and offshore directions. The transect length and spacing are user-specified (white lines Figure 1b; Ferreira & Cooley, 2013).
3. Generate point features along each transect: The onshore direction of the transect is identified by examining the classifications of the raster cells around the marsh-water interface. Point features are generated along the onshore side at the user-specified interval (white dots Figure 1c).
4. Calculate wave height transmission: For each transect, starting at the point closest to the marsh-water interface, the amount of wave height transmission is calculated at each point feature as follows:

$$W_{T,1} = W_{T,0}\, e^{-kx} \qquad \text{(Eq. 2)}$$

Where 1 and 0 subscripts denote the point on the transect closer to onshore and offshore, respectively, and x is the distance between the two points. The classification of the onshore point location

164 determines the k-value used (*e.g.* the yellow and green areas have different k-values in Figure 1).
165 The information is passed down each point on the transect so that the previous $W_{T,1}$ becomes $W_{T,0}$
166 (shaded dots Figure 1d).

167 5. Repeat Step 4 for each transect (Figure 1e).
168 6. Remove point clustering: The ends of transects along a convex coast can become bunched together.
169 To reduce point-clustering, points closer than half the point-spacing interval are compared in a pair-
170 wise fashion. The point farther from the marsh-water interface is removed. This process continues
171 until all points remaining are separated by at least half the point-spacing interval. This step is op-
172 tional and is only performed if this user has the Advanced ArcGIS license.

173

174

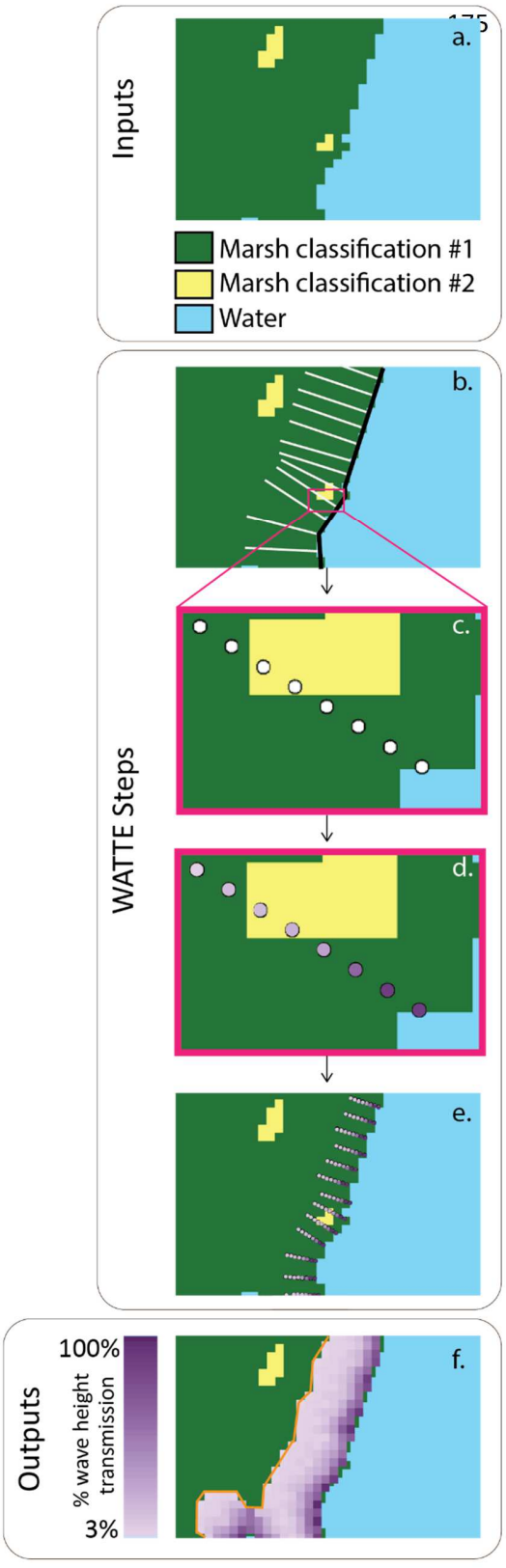

Figure 1: Required inputs, steps of the algorithm, and outputs for WATTE. Parts a through f are a generic example and illustrate the process. Areas in blue are water, and areas in green and yellow are two different marsh classifications. Please refer to Section 3.1 for details.

7. Interpolate the W_T values of all points: Inverse distance weighting or kriging is used to interpolate between all points (Figure 1f). The interpolation method is selected by the user. The underlying equation (Eq. 2) is one-dimensional, but by executing it at many points and interpolating between them, the results appear two-dimensional.

- Outputs: The outputs are a raster of the percent wave height transmission and if the user has the Advanced license of ArcGIS, a polyline bounding the area of wave influence (*i.e.* complete attenuation line, orange line Figure 1f).

Each run of the WATTE toolbox simulates one set of conditions. We recommend performing multiple runs, altering the exponential decay constants each time, to study a variety of conditions and bound the wave attenuation estimates.

3.2. Wave Attenuation Toolbox Development

3.2.1. Inputs

The cells of the input raster must be classified as marsh, water, or other (examples shown in Figure 1a and Figure 3). Marsh is defined as vegetated areas within the intertidal zone, and water is defined as areas within or below the intertidal zone that are void of vegetation. "Other" can be any non-inundated landcover, such as forest or upland that is elevated above the tidal prism. At a minimum, the raster must contain two classifications, marsh and water, but there can be unlimited classifications within the three categories of marsh, water, and other. Classifications could correspond to any characteristics, such as different vegetation species or different levels of biomass productivity. Possible sources of input rasters include the National Wetland Inventory (NWI), data from remote sensing, or the output of land evolution models (*e.g*. marsh migration models like Hydro-MEM (Alizad, Hagen, Morris, Bacopoulos, et al., 2016) and SLAMM (Park et al., 1986)). NWI maps and output from marsh migration models have the advantage of already being classified. Data from remote sensing needs to be processed to classify each raster cell, and there are existing methods for doing so (*e.g.* Farris et al., 2019; Ozesmi & Bauer, 2002). The raster is not required to be a digital elevation model (DEM) or to contain any elevation information. For the current version of WATTE, each marsh classification must be assigned an exponential decay constant, k, which is input by the user. Ideally, k should be calculated from measurements of wave attenuation at the site or an area with similar characteristics. If limited site information is available, the guidance table described in Section 3.3 can be used to set the values.

Although the transects are generated within the toolbox, the user must specify the length of the transects, the distance between them, and the spacing of points along the transect. Figure 2 shows a screenshot of the WATTE user interface, where this information is specified by the user. The spacing of the transects and of the points should be determined by the site characteristics and the resolution of the raster. If a site has many different marsh classifications, closer spacing is needed as compared to a site with only one or two marsh classifications. One point per raster cell is generally recommended. To be conservative, the total length of the transect should be longer than what is expected for complete attenuation. For example, if observations at the site indicate wave action dies off about 100 m into the marsh, then the transects should be at least 120 m, 20% greater.

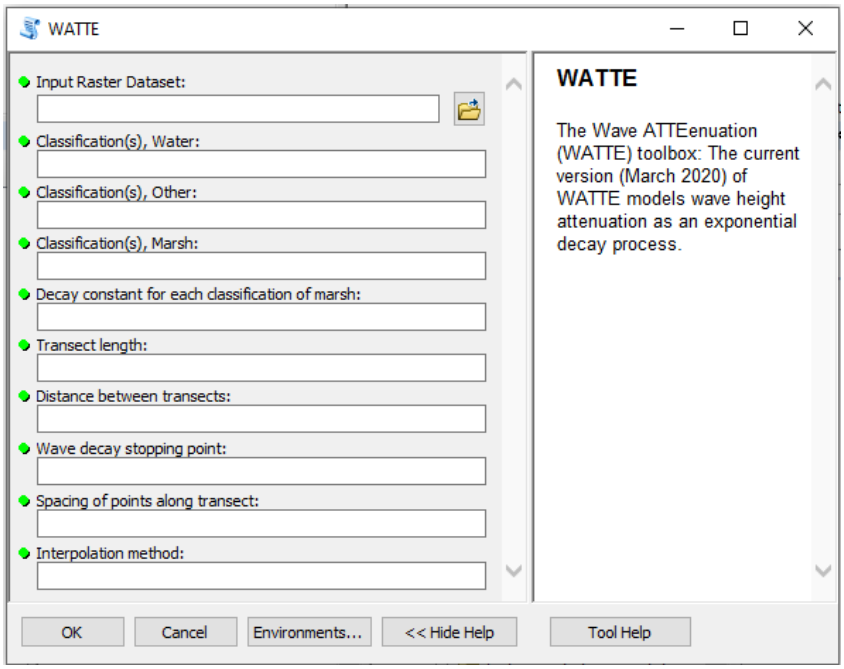

Figure 2: The user interface for the WATTE toolbox. Instructions for each input appear in the right panel as the user clicks through. The inputs shown are described in Section 3.2.1.

The wave calculation (Step 4) will continue moving inland along the points on the transect until one of the following occurs: wave transmission, $W_{T,1}$ (Eq. 1), is below the user-defined threshold; the transect point is on a non-marsh raster cell; or the full length of the transect is reached. In the example shown in Figure 1, the wave transmission threshold is 3%. In other words, once the wave height is attenuated by 97%, the wave is considered completely attenuated and further decrease in wave height is not calculated. There is no information on bathymetry or topography within WATTE, and all areas classified as marsh are possible areas for wave propagation. This simplification implies the water level scenario should be sufficient to fully inundate the marsh, so the waves could theoretically propagate throughout the marsh.

3.2.2. Outputs

The WATTE outputs are a raster of wave height transmission (*i.e.* the percent of original wave height) and the complete attenuation line. This line demarks the extent of wave exposure onshore. If the wave transmission reaches the threshold, the "wave" is considered completely attenuated, and the complete attenuation line is generated. Any marsh farther onshore is not considered to be influenced by wave action. The absence of this line in an area indicates it is within wave exposure. If the user does not have the Advanced ArcGIS license, the complete wave attenuation line must be generated manually using the WATTE output raster. Instructions for manually producing this line are included with the code.

The output raster values are 100% at the marsh-water interface and decrease moving inland. This percentage of wave height transmission can then be multiplied by an initial wave height to show the attenuation in terms of wave height. While two locations may have the same transmission percentage, they may not experience the same wave energy due to their location within the area. Shores exposed to greater fetch are likely to receive larger waves as compared to more sheltered areas. The transmission calculation does not consider whether the area is exposed or sheltered.

3.2.3. Assumptions and Uncertainty

Within WATTE, it is assumed that wave height transformation through vegetation can be modeled as an exponential decay (addressed in Section 2.1) and that waves are parallel to the marsh-water interface. The second assumption is common in attenuation field measurements when the measurement locations

can be selected to better ensure it is true (*i.e.* locations where the bed slope does not vary greatly in the cross-shore direction). Here, we extende it to all points along the marsh-water interface, which includes coastlines with small channels. Wave attenuation results in these areas should be interpreted cautiously. Due to limited fetch, it is unlikely that narrow channels contain sizable waves; however, flow in marsh channels does tend to be perpendicular to the marsh edge (Temmerman et al., 2012), which supports applying this assumption.

WATTE has three main types of uncertainty: initial conditions, model, and parameter (Dietze, 2017). Initial condition uncertainty refers to how accurately the input raster represents conditions on the ground. This uncertainty will vary greatly if the input is based on past or current conditions versus projected future conditions. The model uncertainty is set by the formulation chosen for WATTE, exponential decay. This model was chosen in part because it minimizes the number of parameters, thereby constraining the parameter uncertainty. We focus on parameter uncertainty for the remainder of the document because it comes from the choice of the exponential decay constant, k, which users can manipulate easily.

3.3. Selection of Exponential Decay Constants

As described in Section 3.2.1, an exponential decay constant is required for each marsh classification. The following guidance table is provided to aid with this selection when wave attenuation measurements or observations are not available (Table 1). Since k is the only parameter in the exponential decay model, it contains all of the complexity of vegetation-wave interactions that causes differences in wave attenuation. For this recommendation table, we distilled this complexity to two metrics: biomass and inundation; both are often reported as influencing wave attenuation capacity (Shepard et al., 2011).Within each of these two metrics, there are three classes (low, medium, and high), creating a total of nine values of k.

Biomass is influenced by a range of factors; the low, medium, and high biomass categories capture differences due to physical, biological, and geochemical processes. For example, seasonal shifts (Schoutens et al., 2019), differing hydroperiods (Morris et al., 2002), and subsurface characteristics (Wilson et al., 2015) have all been shown to create differences in biomass productivity and are represented by this metric.

The inundation metric does not refer to the hydroperiod, but rather, to the water depth at which the model will be run. Low inundation is when the water depth is low relative to the height of the vegetation, and the vegetation remains emergent. At the other end, high inundation is when the vegetation is deeply submerged. Ratios of vegetation height to water depth (h_{water}/h_{veg}) have been given for each category to guide the selection.

To populate Table 1, we compiled measured values of k from field studies of species within the *Spartina* genus. Due to limited data availability, all species within the *Spartina* genus are grouped together. While there are many non-*Spartina* species in marshes, there is more available *Spartina* data because this vegetation is common in the low marsh and interacts with waves. Laboratory studies were excluded because by design they often do not capture all of the physical processes at work.

The available studies were sorted as containing low, medium, or high biomass density. The decay constants in each biomass category were informed by three studies (cited in Table 1). Web Plot Digitizer (Rohatgi, 2018) was used to extract data from published figures. The results from each study were organized by increasing water depth to vegetation height ratio. If this information was not provided, the ratio was calculated from the given vegetation height, water depth, and/or site slope, even if the given values were averages. The measured values of k were averaged in each of the nine categories to provide the recommendations. There is an upper limit of 4 for the ratio of water depth to vegetation height. There are limited measurements beyond this depth, as the impact of vegetation diminishes when deeply submerged. The k-values provided span a wide range; using the values for medium biomass, the distance of marsh needed to reach 50% attenuation (*i.e.* half the wave height at the shoreline) varies from 13 m to 116 m for low and high inundation conditions, respectively.

To be clear, Table 1 is not required to run WATTE. The user can input any value for the exponential decay constant. We recommend using location-specific data, if it is available. Regardless of the source of the values, we suggest performing multiple runs using the upper and lower bounds of probable values. For example, the combination of low productivity and high inundation gives the lowest amount of wave attenuation, the most conservative result.

Table 1: Guidance table for the selection of decay constants. Each of the nine categories contains the exponential decay constant, k [1/m], which is the mean of the literature values; the number of data points used in the mean, n; and the inter-quartile range, IQR. [a] The studies used to inform the low-biomass values are Coulombier et al., 2012; Foster-Martinez et al., 2018 (win-

*ter dataset); Paquier et al., 2016. [b] The studies used to inform the medium-biomass values are Foster-Martinez et al., 2018 (summer dataset); I. Möller, 2006; Ysebaert et al., 2011. [c] The studies used to inform the high-biomass values are Jadhav & Chen, 2013; Knutson et al., 1982; Yang et al., 2012. [#]The number of data points is 2, making the IQR simply the difference between the values. *No data was available for high biomass-high inundation conditions, and the value was selected based on the trend for high biomass in the low and medium inundation categories.*

		Inundation Level								
		Low			**Medium**			**High**		
	h_{water}/h_{veg}	<1			≥1 & <2			≥2 & <4		
		$k\ [1/m]$	n	**IQR**	$k\ [1/m]$	n	**IQR**	$k\ [1/m]$	n	**IQR**
Biomass Level	**Low**[a]	0.035	2	0.001[#]	0.021	19	0.011	0.001	12	0.004
	Medium[b]	0.055	7	0.059	0.030	10	0.035	0.006	5	0.010
	High[c]	0.107	6	0.121	0.090	14	0.120	0.015*	-	-

4. Examples of WATTE Application

4.1. Example 1: Validation of Exponential Decay Constant Selection

The performance of WATTE results heavily depends on the selection of the exponential decay constants. In an effort to validate the provided guidance table, the values of k for the following example were selected from Table 1 and were based on a description of vegetation and measurement conditions alone. The results are then compared to the measured wave attenuation at the site.

Morgan et al. (2009) examined differences in functions between meadow and fringing salt marshes in Maine and New Hampshire, US. We use their measurements of wave attenuation at the Mousam River site, where the low marsh is dominated by *Spartina alterniflora*. These measurements were not used to inform the values in Table 1, making it an independent validation. To apply WATTE, we acquired an aerial image from 2009 of the study area taken by the National Agriculture Imagery Program (NAIP). The image was classified with a K-means approach (Duda & Canty, 2002) using Earth Resources Data Analysis System (ERDAS) IMAGINE software (*ERDAS Imagine*, 2018). By visual inspection, we determined that classifying the image with five categories accurately distinguished water, marsh, and non-marsh.

The five classes included two classes that were judged to be water, two classes of marsh, and one class of non-marsh (Figure 3). We selected two sets of k-values to bound the wave attenuation estimate. Informed by descriptions of the vegetation and of the site given in Morgan et al. (2009), the biomass level

of the two marsh classes was varied, and the inundation level was kept the same (Table 2). We estimated the marsh class along the perimeter of the area to be higher productivity than the marsh class more common in the interior. For the wave-height transmission calculation, points were generated every 1 m along each transect due to the NAIP image resolution of 1 m. The transects were set to be 100 m long and to occur every 10 m along the marsh-water interface.

The average of three wave attenuation measurements were provided in Morgan et al. (2009). The results from WATTE were extracted at the measurement location for comparison. The measured wave height decreased from an average of 10.9 cm at the shore to 8.4 cm at a point 5 m from the marsh edge, giving a wave height transmission of 77% (Morgan et al., 2009). Using WATTE, the lower estimate of wave-height transmission (higher attenuation) was 73%, and the upper estimate was 84%, accurately bounding the measured value. This result demonstrates the utility of the Table 1, as well as the necessity of running multiple cases to provide bounds on the results. Note, this case is over a short distance of 5 m. The estimated distance needed to decay to a wave height of 5 cm, about 46% of original wave height, is 12 m for the upper bound and 21 m for the lower bound.

Table 2: Comparison measured and estimated percent of wave height transmission at Mousam River, ME.

Case		**Exponential Decay Constant $k\ [1/m]$**		**Transmission of Wave Height (%)**
Morgan et al. (2009)		--		77%
WATTE Lower Bound	Marsh Class 1	High Biomass Medium Inundation	0.09	73%
	Marsh Class 2	Medium Biomass Low Inundation	0.055	
WATTE Upper Bound	Marsh Class 1	Medium Biomass Medium Inundation	0.03	84%
	Marsh Class 2	Low Biomass Low Inundation	0.035	

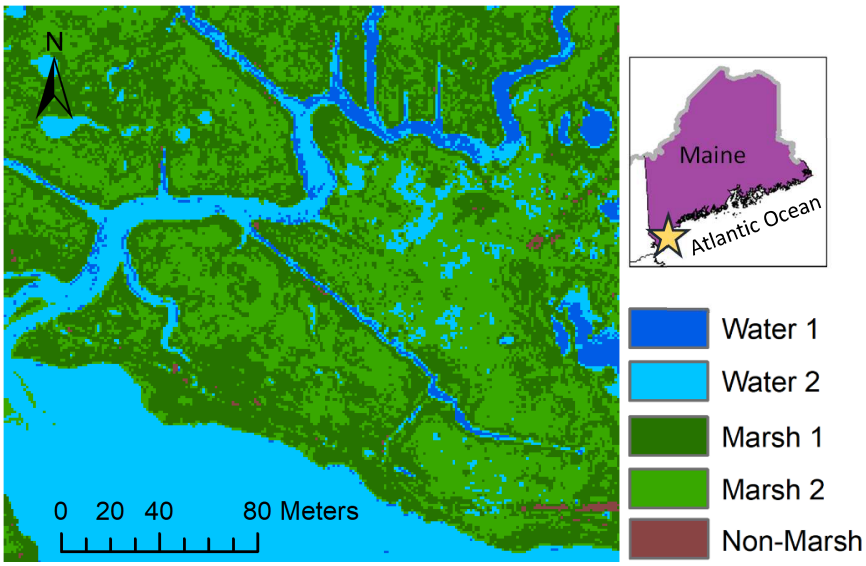

344

345

Figure 3: NAIP aerial imagery (1 m resolution) of a section of the salt marsh at the Mousam River, Maine US (yellow star). The image was classified using ER-DAS Imagine software with five classes.

4.2. Example 2: Application to Grand Bay, USA

WATTE can be applied to large areas of coast. In this example, WATTE was used to analyze 274 km of marsh-water interface in the Grand Bay estuary, which spans Mississippi and Alabama in the US. The input raster is the output from Hydro-MEM (Alizad et al., 2018). Hydro-MEM is a marsh migration model; it couples ADCIRC, a hydrodynamic model, with the Marsh Equilibrium Model (MEM), a biological model, to project maps of marsh productivity (Alizad et al., 2016a; Alizad et al., 2016b). The Hydro-MEM maps show five area classifications: water; upland, which is land elevated above the tidal prism; and low, medium, and high productivity marsh.

Exponential decay constants were selected to simulate conditions at mean higher high water (MHHW) and were based on vegetation and elevation measurements taken to run Hydro-MEM. The results show that complete attenuation is reached about 70 m into the vegetated marsh (Figure 4). This high rate of attenuation can be attributed to the high productivity vegetation along the marsh-water interface. However, many small islands or marsh fragments are less than 70 m wide and are completely subjected to wave action. The wave action varies throughout the estuary with more exposed areas having a longer fetch and receiving larger waves. The marsh in the western portion is more protected than the eastern side, and the waves will differ even if the wave transmission percentage is the same. If typical wave heights are known for the different areas, the percentages of wave transmission can be converted to wave heights by multiplying them by the known wave height or wave statistic (*i.e.* root-mean-square or significant wave height) at the shoreline. Note, these results have not been validated with in-situ measurements, but rather, are provided to show that WATTE can be applied at larger scales. Stakeholders can gain more information from the Hydro-MEM results by using them in WATTE.

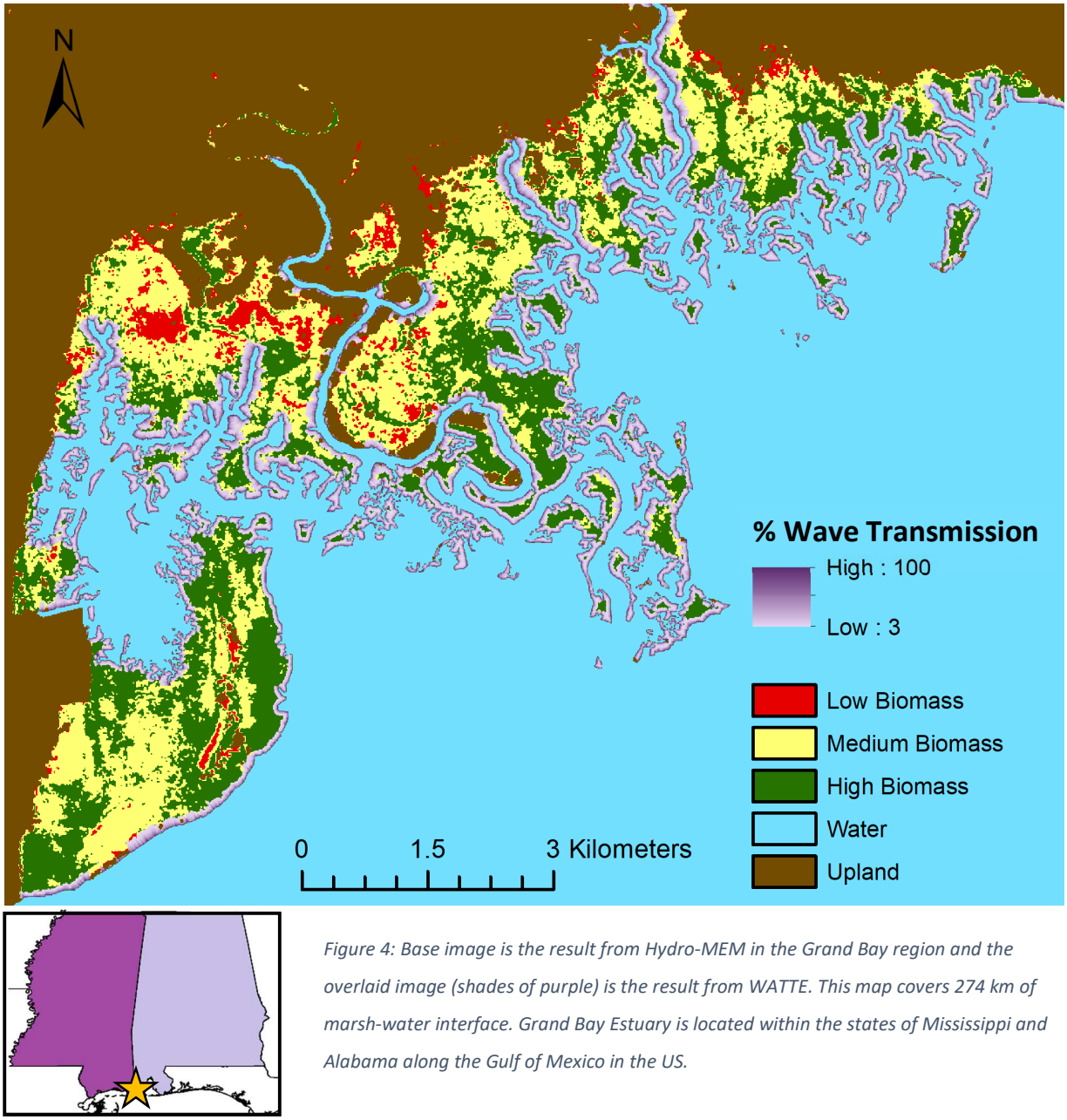

Figure 4: Base image is the result from Hydro-MEM in the Grand Bay region and the overlaid image (shades of purple) is the result from WATTE. This map covers 274 km of marsh-water interface. Grand Bay Estuary is located within the states of Mississippi and Alabama along the Gulf of Mexico in the US.

368

369 **4.3. Example 3: Projections with Future Sea-Level Rise**

370 There is a large effort in the scientific community to understand and predict marsh change with sea-level
371 rise (SLR) and other future environmental conditions (Passeri et al., 2015; Schuerch et al., 2018 and ref-
372 erences therein). As marshes change, the associated ecosystem services also change. Applying WATTE to

373

374

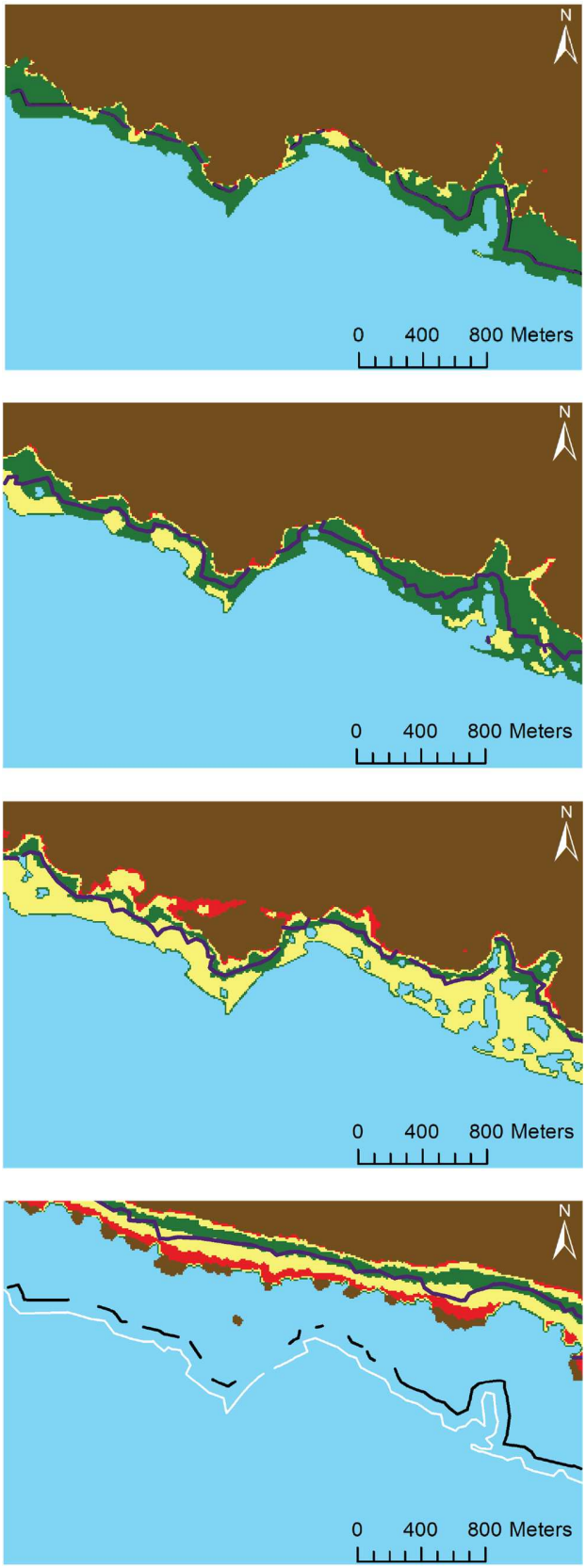

Figure 5: The base images are results from Hydro-MEM for a section of Grand Bay, AL. The results are from (a) 2010 with no SLR; 2050 with (b) intermediate-high SLR and (c) with high SLR; and (d) 2100 with high SLR. The purple line in all images indicates the line of complete attenuation, the extent of wave influence. White arrows in b and c indicate areas of upland exposed to wave action that are likely erosion-prone. White and black lines in d are the 2010 shoreline and line of complete attenuation, respectively. Please refer to the legend in Figure 4 for explanation of the colors.

these future projections allows for better understanding of how the ecosystem service of wave attenuation will change in the future.

Hydro-MEM is one example of a model that projects marsh migration with SLR. We applied WATTE to Hydro-MEM results from intermediate-high and high rates of SLR in an area of Grand Bay, Alabama (Alizad et al., 2018). The complete attenuation line is shown for years 2010 (Figure 5a, no SLR), 2050 (Figure 5b, intermediate-high SLR; Figure 5c, high SLR) and 2100 (Figure 5d, high SLR). The rate of SLR impacts the marsh migration pattern, and therefore, the wave attenuation pattern. With intermediate-high SLR in 2050, the marsh retains high productivity, but the width of marsh narrows. For high SLR in 2050 and 2100, the marsh is largely composed of low productivity biomass; however, it increases in width, and the inland portions of marsh are not as exposed to wave action. The areas where the upland is exposed to wave action (indicated by white arrows in Figure 5) are more erosion-prone and could be areas of targeted intervention. Figure 5d shows the marsh edge and complete attenuation line for 2010 overlaid on the high SLR results for 2100. The marsh retreat is apparent, as well as the widening of the area influenced by waves.

Hydro-MEM results (Alizad et al., 2018) show that ponding occurs with high SLR in 2050 (Figure 5c). The edges of these ponds are considered part of the marsh-water interface and are treated the same as the marsh-water interface at the shoreline. Although waves being generated in interior ponds are likely small, previous studies have shown that wind-generated shear stresses can lead to pond expansion, and therefore, pond edges are included in WATTE (Day et al., 2011).

5. Discussion

5.1. Evaluation of WATTE as a Participatory Modeling Tool

By focusing on only the process of wave attenuation through marsh vegetation, WATTE can be used within a variety of assessment methodologies and modeling frameworks. Its simplicity makes it suitable for participatory modeling, where stakeholders are formally engaged in problem identification and analysis (Voinov et al., 2018). Due to the opportunity to learn and revise through process iteration, participatory modeling is well-suited for addressing complex, environmental-management decisions (Stave, 2010), such as coastal protection plans and restoration activities. Tool selection should be tailored for the particular project and stakeholders, as it is an important step in a successful application of the participatory modeling process (Voinov & Bousquet, 2010).

Voinov et al. (2018) compared 17 types of participatory modeling tools grouped by four modeling methods; GIS was categorized as a quantitative modeling method with aggregated results. Compared to other tools, the greatest strength of GIS was the ability to represent spatial results, as could be expected. It was also judged to be strong in ease of communication and modification. GIS tended to be weak in areas where many tools were weak, such as in handling uncertainty and representing temporal results (Voinov et al., 2018). We address the lack of uncertainty by recommending users run WATTE multiple times to bound the results. Temporal results can be achieved, if data throughout landscape changes is available WATTE input; the time scale would then be that of the land evolution changes.

We evaluated WATTE based on the eight criteria detailed in Bagstad et al. (2013) (Table 3). These criteria were developed to evaluate the usability of decision-support tools for quantification of ecosystem services and have been used to evaluate tools similar to WATTE. Overall, WATTE performs well, as it is publicly available and provides quantitative results. It can be applied to a wide range of spatial scales; increasing the scale simply increases the run time. Since it requires ArcGIS software, we judged it to be moderate cost. It does not have a valuation component, and it would therefore need to be used in conjunction with another tool in order to make economic assessments (see Barbier et al. (2013) for an example). We expect WATTE to be useful for a range of groups performing research at the coastal land margin and interested in assessing patterns of wave attenuation by coastal vegetation, including academic institutions, industry, community groups, and non-profits (*e.g.* The Nature Conservancy, Climate Central).

Table 3: Application of evaluation criteria from Bagstad et al. (2013) to WATTE

Criteria from Bagstad et al. (2013)	**WATTE**
Quantification and Uncertainty	Quantitative; uncertainty can be determined by varying inputs
Time Requirements	Low to Medium, depending on availability of existing data
Capacity for Independent Application	Yes, if user has access to ArcGIS
Level of Development and Documentation	Fully documented with examples
Scalability	Multiple scales
Generalizability	High, within vegetated shorelines

Nonmonetary and Cultural Perspectives	No valuation component
Affordability, Insights, and Integration with existing environmental assessment	Useful as a moderate-cost estimation of wave attenuation

5.2. Strengths and Limitations

A core strength of WATTE is that it can provide reasonable estimates of wave attenuation with limited information. As illustrated in Example 1 (Section 4.1), the input raster can be derived from remote sensing data, which is more available for coasts across the globe as compared to in-situ measurements. Remote sensing is a valuable resource for work in under-studied locations and is gaining recognition for its usefulness in wetland restoration and management (Ganju, 2019). The exponential decay constants can be sourced from measurements in a different area with similar conditions, and they can be varied in multiple runs of WATTE to test bounding cases. Having only one parameter to manipulate simplifies this process. Of course, the more that is known about a site, the more can be done with the WATTE results. For example, converting from percentages of wave transmission to wave heights requires an understanding of typical wave conditions throughout the site. It should be noted that users must be careful not to extrapolate results to extreme conditions (*e.g.* storm surge), unless data from these conditions was used to calculate the exponential decay constants.

The benefit of flexibility also comes at the price of not being mechanistic. In the measurements of exponential decay constants, all processes are bundled together. For example, if the stem density changes, that parameter cannot be adjusted independently the way it can be in a drag model. The same is true for changes in slope, which impact shoaling and bed friction processes. Instead of being directly adjusted, the effect of these changes on the exponential decay constant first needs to be judged.

Similarly, not requiring a DEM, or any elevation information, removes a barrier to usage, but it creates additional factors to consider in the interpretation of the results. As stated in Section 3.2.1, wave propagation can occur in any area classified as marsh and cannot occur in areas classified as “other.” That is why it is important to run a scenario where the marsh is fully inundated or to designate non-inundated marsh areas as “other.” If running a low inundation scenario, unrealistic wave propagation could occur where the marsh is dry. This result is likely not common because high attenuation occurs at low inundation, and waves are often completely attenuated before reaching higher elevations. Another limitation is

that each transect is independent. There is no interaction between waves along different transects, even if those transects overlap. When points along different transects are clustered together, the points closer to the marsh-water interface are preferentially kept in the interpolation to produce a conservative estimate of attenuation (Step 6 in Section 3.1).

5.3. Future Applications

Wave attenuation is just one of many ecosystem services performed by marshes. Coastal projects incorporating marshes as NNBFs are widely promoted (Bridges et al., 2015; Shepard et al., 2011; Sutton-Grier et al., 2018), yet to properly evaluate NNBFs against other options, formal recognition of the ecosystem services is necessary (Sutton-Grier et al., 2015). WATTE can quantify the service of wave attenuation to provide a more complete picture. Future iterations of WATTE can expand applicable shoreline types. The exponential decay model is appropriate for some; for example, Pinsky et al., (2013) calculated exponential decay constants for previous studies of wave attenuation through kelp, mangroves, and seagrasses, and Lacy & MacVean (2016) found wave attenuation over mudflats follows exponential decay with decay constants that are inversely related to depth squared. However, it is likely other models will need to be added to WATTE to address all shorelines of interest. Since the code is open source, we are hopeful others will modify and improve it to suit particular project needs.

6. Conclusions

The accelerating rate of sea level rise creates additional impetus to study how coastlines will change and to communicate the findings to a broader audience. It is important to communicate not only how marshes will change, but also, how the associated ecosystem services will change, some of which may have direct impacts on the lives of coastal residents. Here, we focus on wave attenuation by marsh vegetation and have presented an ArcGIS toolbox, WATTE, to estimate wave height transmission along any given marsh shoreline. While vegetation-wave interaction is highly complex, there is a general consensus that wave heights exponentially decay as they pass through or over vegetation (Tempest et al., 2015 and references therein). We model wave attenuation as an exponential decay to keep the process and its application simple. WATTE can be applied to create location-specific estimates without extensive field measurements or advanced numerical models. The results from WATTE add information to existing datasets, enhancing their value. These datasets may be sourced from observations collected previously, current data, or projections of future conditions. Datasets can also be manipulated to reflect anticipated changes resulting from coastal projects, and the results can help evaluate these projects, estimating

their impact on wave energy at the site. This information can be used to identify priority areas for conservation and restoration.

Acknowledgements

This work was supported by Awards No. NA10NOS4780146 and NA16NOS4780208 from the National Oceanic and Atmospheric Administration (NOAA) Ecological Effects of Sea Level Rise (EESLR) Program and the Louisiana Sea Grant Laborde Chair. The authors would like to acknowledge Dr. Denise DeLorme for assistance with the literature review, as well as W. Ryan Lauve for classifying the NAIP imagery. The manuscript significantly benefited from three anonymous reviews. The statements and conclusions do not necessarily reflect the views of NOAA-EESLR, Louisiana Sea Grant, Louisiana State University, University of South Carolina, or their affiliates.

Declaration of interests: None

496 **References**
497
498 Abuodha, P. A. W., & Kairo, J. G. (2001). Human-induced stresses on mangrove swamps along the Ken-
499 yan coast. *Hydrobiologia*, *458*(1), 255–265. https://doi.org/10.1023/A:1013130916811
500 Alizad, K., Hagen, S. C., Morris, J. T., Bacopoulos, P., Bilskie, M. V., Weishampel, J. F., & Medeiros, S. C.
501 (2016). A coupled, two-dimensional hydrodynamic-marsh model with biological feedback. *Eco-*
502 *logical Modelling*, *327*, 29–43. https://doi.org/10.1016/j.ecolmodel.2016.01.013
503 Alizad, K., Hagen, S. C., Morris, J. T., Medeiros, S. C., Bilskie, M. V., & Weishampel, J. F. (2016). Coastal
504 wetland response to sea-level rise in a fluvial estuarine system: WETLAND RESPONSE TO SLR.
505 *Earth's Future*, *4*(11), 483–497. https://doi.org/10.1002/2016EF000385
506 Alizad, K., Hagen, S. C., Medeiros, S. C., Bilskie, M. V., Morris, J. T., Balthis, L., & Buckel, C. A. (2018). Dy-
507 namic responses and implications to coastal wetlands and the surrounding regions under sea
508 level rise. *PLOS ONE*, *13*(10), e0205176. https://doi.org/10.1371/journal.pone.0205176
509 ArcGIS. (2018). (Version Version 10.6). Redlands, CA USA: Environmental Systems Research Insitute, Inc.
510 Bagstad, K. J., Semmens, D. J., Waage, S., & Winthrop, R. (2013). A comparative assessment of decision-
511 support tools for ecosystem services quantification and valuation. *Ecosystem Services*, *5*, 27–39.
512 https://doi.org/10.1016/j.ecoser.2013.07.004
513 Barbier, E. B., Georgiou, I. Y., Enchelmeyer, B., & Reed, D. J. (2013). The Value of Wetlands in Protecting
514 Southeast Louisiana from Hurricane Storm Surges. *PLoS ONE*, *8*(3), e58715.
515 https://doi.org/10.1371/journal.pone.0058715
516 Bridges, T. S., Burks-Copes, K. A., Bates, M. E., Collier, Z. A., Fischenich, J. C., Piercy, C. D., et al. (2015).
517 *Use of natural and nature-based features (NNBF) for coastal resilience*. US Army Engineer Re-
518 search and Development Center, Environmental Laboratory ….

519 Coulombier, T., Neumeier, U., & Bernatchez, P. (2012). Sediment transport in a cold climate salt marsh
520 (St. Lawrence Estuary, Canada), the importance of vegetation and waves. *Estuarine, Coastal and*
521 *Shelf Science*, *101*, 64–75. https://doi.org/10.1016/j.ecss.2012.02.014
522 Crosby, S. C., Sax, D. F., Palmer, M. E., Booth, H. S., Deegan, L. A., Bertness, M. D., & Leslie, H. M. (2016).
523 Salt marsh persistence is threatened by predicted sea-level rise. *Estuarine, Coastal and Shelf Sci-*
524 *ence*, *181*, 93–99. https://doi.org/10.1016/j.ecss.2016.08.018
525 Dalrymple, R. A., Kirby, J. T., & Hwang, P. A. (1984). Wave Diffraction Due to Areas of Energy Dissipation.
526 *Journal of Waterway, Port, Coastal, and Ocean Engineering*, *110*(1), 67–79.
527 https://doi.org/10.1061/(ASCE)0733-950X(1984)110:1(67)
528 Day, J. W., Kemp, G. P., Reed, D. J., Cahoon, D. R., Boumans, R. M., Suhayda, J. M., & Gambrell, R. (2011).
529 Vegetation death and rapid loss of surface elevation in two contrasting Mississippi delta salt
530 marshes: The role of sedimentation, autocompaction and sea-level rise. *Ecological Engineering*,
531 *37*(2), 229–240. https://doi.org/10.1016/j.ecoleng.2010.11.021
532 Dietze, M. C. (2017). *Ecological forecasting*. Princeton University Press.
533 Doughty, C. L., Cavanaugh, K. C., Hall, C. R., Feller, I. C., & Chapman, S. K. (2017). Impacts of mangrove
534 encroachment and mosquito impoundment management on coastal protection services. *Hydro-*
535 *biologia*, *803*(1), 105–120. https://doi.org/10.1007/s10750-017-3225-0
536 Duarte, C. M., Losada, I. J., Hendriks, I. E., Mazarrasa, I., & Marbà, N. (2013). The role of coastal plant
537 communities for climate change mitigation and adaptation. *Nature Climate Change*, *3*(11), 961–
538 968. https://doi.org/10.1038/nclimate1970
539 Duda, T., & Canty, M. (2002). Unsupervised classification of satellite imagery: Choosing a good algo-
540 rithm. *International Journal of Remote Sensing*, *23*(11), 2193–2212.
541 https://doi.org/10.1080/01431160110078467
542 ERDAS Imagine. (2018). (Version 16.5). Madison, AL USA: Hexagon Geospatial.

543 Farris, A. S., Defne, Z., & Ganju, N. K. (2019). Identifying Salt Marsh Shorelines from Remotely Sensed
544 Elevation Data and Imagery. *Remote Sensing*, *11*(15), 1795. https://doi.org/10.3390/rs11151795
545 Ferreira, M., & Cooley. (2013). *Perpendicular Transects*. Retrieved from http://gis4geomorphol-
546 ogy.com/stream-transects-partial/
547 Foster-Martinez, M. R., Lacy, J. R., Ferner, M. C., & Variano, E. A. (2018). Wave attenuation across a tidal
548 marsh in San Francisco Bay. *Coastal Engineering*, *136*, 26–40.
549 https://doi.org/10.1016/j.coastaleng.2018.02.001
550 Ganju, N. K. (2019). Marshes Are the New Beaches: Integrating Sediment Transport into Restoration
551 Planning. *Estuaries and Coasts*. https://doi.org/10.1007/s12237-019-00531-3
552 Gedan, K. Bromberg, Silliman, B. R., & Bertness, M. D. (2009). Centuries of Human-Driven Change in Salt
553 Marsh Ecosystems. *Annual Review of Marine Science*, *1*(1), 117–141.
554 https://doi.org/10.1146/annurev.marine.010908.163930
555 Gedan, Keryn B., Kirwan, M. L., Wolanski, E., Barbier, E. B., & Silliman, B. R. (2011). The present and fu-
556 ture role of coastal wetland vegetation in protecting shorelines: answering recent challenges to
557 the paradigm. *Climatic Change*, *106*(1), 7–29. https://doi.org/10.1007/s10584-010-0003-7
558 Guannel, G., Ruggiero, P., Faries, J., Arkema, K., Pinsky, M., Gelfenbaum, G., et al. (2015). Integrated
559 modeling framework to quantify the coastal protection services supplied by vegetation. *Journal*
560 *of Geophysical Research: Oceans*, *120*(1), 324–345. https://doi.org/10.1002/2014JC009821
561 Guannel, G., Arkema, K., Ruggiero, P., & Verutes, G. (2016). The Power of Three: Coral Reefs, Seagrasses
562 and Mangroves Protect Coastal Regions and Increase Their Resilience. *PLOS ONE*, *11*(7),
563 e0158094. https://doi.org/10.1371/journal.pone.0158094
564 Hijuelos, A. C., Dijkstra, J. T., Carruthers, T. J. B., Heynert, K., Reed, D. J., & van Wesenbeeck, B. K. (2019).
565 Linking management planning for coastal wetlands to potential future wave attenuation under a

range of relative sea-level rise scenarios. *PLOS ONE*, *14*(5), e0216695. https://doi.org/10.1371/journal.pone.0216695

Hughes, T. P., Kerry, J. T., Baird, A. H., Connolly, S. R., Dietzel, A., Eakin, C. M., et al. (2018). Global warming transforms coral reef assemblages. *Nature*, *556*(7702), 492–496. https://doi.org/10.1038/s41586-018-0041-2

Ilman, M., Dargusch, P., Dart, P., & Onrizal. (2016). A historical analysis of the drivers of loss and degradation of Indonesia's mangroves. *Land Use Policy*, *54*, 448–459. https://doi.org/10.1016/j.landusepol.2016.03.010

Jadhav, R. S., & Chen, Q. (2013). Probability distribution of wave heights attenuated by salt marsh vegetation during tropical cyclone. *Coastal Engineering*, *82*, 47–55. https://doi.org/10.1016/j.coastaleng.2013.08.006

Knutson, P. L., Brochu, R. A., Seelig, W. N., & Inskeep, M. (1982). Wave damping inSpartina alterniflora marshes. *Wetlands*, *2*(1), 87–104. https://doi.org/10.1007/BF03160548

Kobayashi, N., Raichle, A. W., & Asano, T. (1993). Wave Attenuation by Vegetation. *Journal of Waterway, Port, Coastal, and Ocean Engineering*, *119*(1), 30–48. https://doi.org/10.1061/(ASCE)0733-950X(1993)119:1(30)

Koch, E. W., Barbier, E. B., Silliman, B. R., Reed, D. J., Perillo, G. M., Hacker, S. D., et al. (2009). Non-linearity in ecosystem services: temporal and spatial variability in coastal protection. *Frontiers in Ecology and the Environment*, *7*(1), 29–37. https://doi.org/10.1890/080126

Komar, P. D. (1998). *Beach processes and sedimentation* (2nd ed). Upper Saddle River, N.J: Prentice Hall.

Lacy, J. R., & MacVean, L. J. (2016). Wave attenuation in the shallows of San Francisco Bay. *Coastal Engineering*, *114*, 159–168. https://doi.org/10.1016/j.coastaleng.2016.03.008

588 Leigh, E. G., Paine, R. T., Quinn, J. F., & Suchanek, T. H. (1987). Wave energy and intertidal productivity.
589 *Proceedings of the National Academy of Sciences*, *84*(5), 1314–1318.
590 https://doi.org/10.1073/pnas.84.5.1314
591 Luettich Jr, R. A., Westerink, J. J., & Scheffner, N. W. (1992). *ADCIRC: An Advanced Three-Dimensional*
592 *Circulation Model for Shelves, Coasts, and Estuaries. Report 1. Theory and Methodology of*
593 *ADCIRC-2DDI and ADCIRC-3DL.* COASTAL ENGINEERING RESEARCH CENTER VICKSBURG MS.
594 Möller, I. (2006). Quantifying saltmarsh vegetation and its effect on wave height dissipation: Results
595 from a UK East coast saltmarsh. *Estuarine, Coastal and Shelf Science*, *69*(3–4), 337–351.
596 https://doi.org/10.1016/j.ecss.2006.05.003
597 Möller, I., & Spencer, T. (2002). Wave dissipation over macro-tidal saltmarshes: Effects of marsh edge
598 typology and vegetation change. *Journal of Coastal Research*, *36*, 506–521.
599 Möller, I., Spencer, T., French, J. R., Leggett, D. J., & Dixon, M. (1999). Wave Transformation Over Salt
600 Marshes: A Field and Numerical Modelling Study from North Norfolk, England. *Estuarine,*
601 *Coastal and Shelf Science*, *49*(3), 411–426. https://doi.org/10.1006/ecss.1999.0509
602 Möller, Iris, Kudella, M., Rupprecht, F., Spencer, T., Paul, M., van Wesenbeeck, B. K., et al. (2014). Wave
603 attenuation over coastal salt marshes under storm surge conditions. *Nature Geoscience*, *7*(10),
604 727–731. https://doi.org/10.1038/ngeo2251
605 Morgan, P. A., Burdick, D. M., & Short, F. T. (2009). The Functions and Values of Fringing Salt Marshes in
606 Northern New England, USA. *Estuaries and Coasts*, *32*(3), 483–495.
607 https://doi.org/10.1007/s12237-009-9145-0
608 Morris, J. T., Sundareshwar, P. V., Nietch, C. T., Kjerfve, B., & Cahoon, D. R. (2002). Responses of Coastal
609 Wetlands to Rising Sea Level. *Ecology*, *83*(10), 2869–2877. https://doi.org/10.1890/0012-
610 9658(2002)083[2869:ROCWTR]2.0.CO;2

Munk, W. H. (1950). ORIGIN AND GENERATION OF WAVES. *Coastal Engineering Proceedings*, *1*(1). https://doi.org/10.9753/icce.v1.1

Narayan, S., Beck, M. W., Reguero, B. G., Losada, I. J., van Wesenbeeck, B., Pontee, N., et al. (2016). The Effectiveness, Costs and Coastal Protection Benefits of Natural and Nature-Based Defences. *PLOS ONE*, *11*(5), e0154735. https://doi.org/10.1371/journal.pone.0154735

Osorio-Cano, J. D., Osorio, A. F., & Peláez-Zapata, D. S. (2017). Ecosystem management tools to study natural habitats as wave damping structures and coastal protection mechanisms. *Ecological Engineering*. https://doi.org/10.1016/j.ecoleng.2017.07.015

Ozesmi, S. L., & Bauer, M. E. (2002). Satellite remote sensing of wetlands. *Wetlands Ecology and Management*, *10*(5), 381–402. https://doi.org/10.1023/A:1020908432489

Paquier, A.-E., Haddad, J., Lawler, S., & Ferreira, C. M. (2016). Quantification of the Attenuation of Storm Surge Components by a Coastal Wetland of the US Mid Atlantic. *Estuaries and Coasts*. https://doi.org/10.1007/s12237-016-0190-1

Park, R. A., Armentano, T. V., & Cloonan, C. L. (1986). Predicting the effects of sea level rise on coastal wetlands. *Effects of Changes in Stratospheric Ozone and Global Climate*, *4*, 129–152.

Passeri, D. L., Hagen, S. C., Medeiros, S. C., Bilskie, M. V., Alizad, K., & Wang, D. (2015). The dynamic effects of sea level rise on low-gradient coastal landscapes: A review. *Earth's Future*, *3*(6), 159–181. https://doi.org/10.1002/2015EF000298

Peruzzo, P., De Serio, F., Defina, A., & Mossa, M. (2018). Wave Height Attenuation and Flow Resistance Due to Emergent or Near-Emergent Vegetation. *Water*, *10*(4), 402. https://doi.org/10.3390/w10040402

Pinsky, M. L., Guannel, G., & Arkema, K. K. (2013). Quantifying wave attenuation to inform coastal habitat conservation. *Ecosphere*, *4*(8), art95. https://doi.org/10.1890/ES13-00080.1

Reeve, D., Chadwick, A., & Fleming, C. (2018). Conceptual and detailed design. In *Coastal engineering* (Third edition, pp. 348–468). Boca Raton: Taylor & Francis, CRC Press.

Roelvink, D., Reniers, A., Van Dongeren, A., De Vries, J. V. T., McCall, R., & Lescinski, J. (2009). Modelling storm impacts on beaches, dunes and barrier islands. *Coastal Engineering*, *56*(11–12), 1133–1152.

Roelvink, D., Reniers, A., Van Dongeren, A., Van Thiel de Vries, J., Lescinski, J., & McCall, R. (2010). XBeach model description and manual. *Unesco-IHE Institute for Water Education, Deltares and Delft University of Tecnhology. Report June*, *21*, 2010.

Rohatgi, A. (2018). WebPlotDigitizer (Version 4.1). San Francisco, California, USA. Retrieved from https://automeris.io/WebPlotDigitizer/

van Rooijen, A. A., van Thiel de Vries, J. S. M., McCall, R. T., van Dongeren, A. R., Roelvink, J. A., & Reniers, A. J. H. M. (2015). Modeling of wave attenuation by vegetation with XBeach (Vol. Institutional Repository). Presented at the E-proceedings of the 36th IAHR World Congress, The Hague, the Netherlands, 28 June-3 July 2015, IAHR.

van Rooijen, A. A., McCall, R. T., van Thiel de Vries, J. S. M., van Dongeren, A. R., Reniers, A. J. H. M., & Roelvink, J. A. (2016). Modeling the effect of wave-vegetation interaction on wave setup: WAVE SETUP DAMPING BY VEGETATION. *Journal of Geophysical Research: Oceans*, *121*(6), 4341–4359. https://doi.org/10.1002/2015JC011392

Ruckelshaus, M. H., Guannel, G., Arkema, K., Verutes, G., Griffin, R., Guerry, A., et al. (2016). Evaluating the Benefits of Green Infrastructure for Coastal Areas: Location, Location, Location. *Coastal Management*, *44*(5), 504–516. https://doi.org/10.1080/08920753.2016.1208882

655 Schoutens, K., Heuner, M., Minden, V., Schulte Ostermann, T., Silinski, A., Belliard, J.-P., & Temmerman,
656 S. (2019). How effective are tidal marshes as nature-based shoreline protection throughout sea-
657 sons?: Tidal marshes as shoreline protection. *Limnology and Oceanography*.
658 https://doi.org/10.1002/lno.11149
659 Schuerch, M., Spencer, T., Temmerman, S., Kirwan, M. L., Wolff, C., Lincke, D., et al. (2018). Future re-
660 sponse of global coastal wetlands to sea-level rise. *Nature*, *561*(7722), 231–234.
661 https://doi.org/10.1038/s41586-018-0476-5
662 Shepard, C. C., Crain, C. M., & Beck, M. W. (2011). The Protective Role of Coastal Marshes: A Systematic
663 Review and Meta-analysis. *PLoS ONE*, *6*(11), e27374. https://doi.org/10.1371/jour-
664 nal.pone.0027374
665 Short, A. D. (2012). Coastal Processes and Beaches. *Nature Education Knowledge*, *3*(10), 15.
666 Stave, K. (2010). Participatory System Dynamics Modeling for Sustainable Environmental Management:
667 Observations from Four Cases. *Sustainability*, *2*(9), 2762–2784.
668 https://doi.org/10.3390/su2092762
669 Sutton-Grier, A. E., & Sandifer, P. A. (2018). Conservation of Wetlands and Other Coastal Ecosystems: a
670 Commentary on their Value to Protect Biodiversity, Reduce Disaster Impacts, and Promote Hu-
671 man Health and Well-Being. *Wetlands*. https://doi.org/10.1007/s13157-018-1039-0
672 Sutton-Grier, A. E., Wowk, K., & Bamford, H. (2015). Future of our coasts: The potential for natural and
673 hybrid infrastructure to enhance the resilience of our coastal communities, economies and eco-
674 systems. *Environmental Science & Policy*, *51*, 137–148. https://doi.org/10.1016/j.en-
675 vsci.2015.04.006
676 Sutton-Grier, A. E., Gittman, R. K., Arkema, K. K., Bennett, R. O., Benoit, J., Blitch, S., et al. (2018). Invest-
677 ing in Natural and Nature-Based Infrastructure: Building Better Along Our Coasts. *Sustainability*,
678 *10*(2), 523. https://doi.org/10.3390/su10020523

679 Suzuki, T., Zijlema, M., Burger, B., Meijer, M. C., & Narayan, S. (2012). Wave dissipation by vegetation
680 with layer schematization in SWAN. *Coastal Engineering*, *59*(1), 64–71.
681 Tallis, H., Ricketts, T., Nelson, E., Ennaanay, D., Wolny, S., Olwero, N., et al. (2010). *InVEST 1.004 beta*
682 *User's Guide. The Natural Capital Project*. Stanford University.
683 Temmerman, S., Moonen, P., Schoelynck, J., Govers, G., & Bouma, T. J. (2012). Impact of vegetation die-
684 off on spatial flow patterns over a tidal marsh. *Geophysical Research Letters*, *39*(3), n/a-n/a.
685 https://doi.org/10.1029/2011GL050502
686 Tempest, J. A., Möller, I., & Spencer, T. (2015). A review of plant-flow interactions on salt marshes: the
687 importance of vegetation structure and plant mechanical characteristics: Salt marsh plant-flow
688 interactions. *Wiley Interdisciplinary Reviews: Water*, *2*(6), 669–681.
689 https://doi.org/10.1002/wat2.1103
690 Voinov, A., & Bousquet, F. (2010). Modelling with stakeholders☆. *Environmental Modelling & Software*,
691 *25*(11), 1268–1281. https://doi.org/10.1016/j.envsoft.2010.03.007
692 Voinov, A., Jenni, K., Gray, S., Kolagani, N., Glynn, P. D., Bommel, P., et al. (2018). Tools and methods in
693 participatory modeling: Selecting the right tool for the job. *Environmental Modelling & Software*,
694 *109*, 232–255. https://doi.org/10.1016/j.envsoft.2018.08.028
695 Waycott, M., Duarte, C. M., Carruthers, T. J. B., Orth, R. J., Dennison, W. C., Olyarnik, S., et al. (2009). Ac-
696 celerating loss of seagrasses across the globe threatens coastal ecosystems. *Proceedings of the*
697 *National Academy of Sciences*, *106*(30), 12377–12381.
698 https://doi.org/10.1073/pnas.0905620106
699 Wiberg, P. L., Taube, S. R., Ferguson, A. E., Kremer, M. R., & Reidenbach, M. A. (2018). Wave Attenuation
700 by Oyster Reefs in Shallow Coastal Bays. *Estuaries and Coasts*. https://doi.org/10.1007/s12237-
701 018-0463-y

Wilson, A. M., Evans, T., Moore, W., Schutte, C. A., Joye, S. B., Hughes, A. H., & Anderson, J. L. (2015). Groundwater controls ecological zonation of salt marsh macrophytes. *Ecology*, *96*(3), 840–849. https://doi.org/10.1890/13-2183.1

Yang, S. L., Shi, B. W., Bouma, T. J., Ysebaert, T., & Luo, X. X. (2012). Wave Attenuation at a Salt Marsh Margin: A Case Study of an Exposed Coast on the Yangtze Estuary. *Estuaries and Coasts*, *35*(1), 169–182. https://doi.org/10.1007/s12237-011-9424-4

Ysebaert, T., Yang, S.-L., Zhang, L., He, Q., Bouma, T. J., & Herman, P. M. J. (2011). Wave Attenuation by Two Contrasting Ecosystem Engineering Salt Marsh Macrophytes in the Intertidal Pioneer Zone. *Wetlands*, *31*(6), 1043–1054. https://doi.org/10.1007/s13157-011-0240-1

van Zanten, B. T., van Beukering, P. J. H., & Wagtendonk, A. J. (2014). Coastal protection by coral reefs: A framework for spatial assessment and economic valuation. *Ocean & Coastal Management*, *96*, 94–103. https://doi.org/10.1016/j.ocecoaman.2014.05.001